Chrysoporthe brasiliensis sp. nov. pathogenic to Melastomataceae in southeast Brazil

Gabrielle Avelar Silva[a], Mara Elisa Soares Oliveira[b], Géssica Mylena Santana Rêgo[a], Brenda D. Wingfield[c], Michael J. Wingfield[c], Maria Alves Ferreira[a]*

[a] Department of Plant Pathology , Universidade Federal de Lavras, 3037, Lavras, Minas Gerais, Brazil

[b] Department of Plant Pathology, Universidade Federal do Tocantins, 66, Gurupi, Tocantins, Brazil

[c] Department of Biochemistry, Genetics and Microbiology, Forestry and Agricultural Biotechnology Institute (FABI), University of Pretoria, 0002, Pretoria, South Africa

*Corresponding author. E-mail address: mariaferreira@ufla.br

ABSTRACT

Species in the Melastomataceae (Myrtales) include trees and woody shrubs that are amongst the most common hosts of *Chrysoporthe* and related fungi. These fungi cause stem cankers, branch death and in extreme cases, kill their hosts. *Chrysoporthe*-like fungi were observed on *Miconia* spp. and *Rhynchanthera grandiflora* (Melastomataceae) plants during tree disease surveys in south-eastern Brazil including the states of Minas Gerais and Rio de Janeiro. The aims of this study were to isolate and identify the fungi utilising morphological characteristics and phylogenetic analyses. This led to the identification of a new species of *Chrysoporthe* described here as *Chrysoporthe brasilensis sp.nov*. Inoculations were conducted on *R. grandiflora* and *M. theaezans*, showing that *C. brasiliensis* is an aggressive pathogen. This study adds to a growing number of reports of new and pathogenic species of *Chrysoporthe* that

potentially threaten native Myrtales globally, including important trees such as *Eucalyptus*, both in natural ecosystems and in planted forests.

Keywords: Cryphonectriaceae; Phylogeny; Canker; Trees; Pathogenicity.

1. Introduction

The Cryphonectriaceae includes some of the most important fungal pathogens of trees. The family is best known for *Cryphonectria parasitica* that devastated natural chestnut (*Castanea dentata*) ecosystems in Europe and North America (Anagnostakis, 1987; Fairchild, 1913; Gryzenhout et al., 2009). In recent years, numerous genera in the Cryphonectriaceae have been discovered in Southern Hemisphere countries, some of which have caused serious damage to plantation-grown *Eucalyptus* (Crous et al., 2012; Gryzenhout et al., 2010; Soares et al., 2018; Wang et al., 2018; Wang et al., 2020; Wingfield, 2003). Of these genera, *Chrysoporthe,* which was previously treated in *Cryphonectria,* has received most attention due to the canker disease that it causes on *Eucalyptus* (Bruner, 1917; Chungu et al., 2009; Gryzenhout et al., 2004; Gryzenhout et al., 2005; Soares et al., 2018). An interesting contemporary discovery has been that many of these fungi occur on native Myrtales, including the Melastomataceae that have undergone host range expansions to infect *Eucalyptus* (Oliveira et al., 2022; van der Merwe et al., 2013; Wingfield et al., 2001).

The Melastomataceae (Myrtales) is represented by approximately 177 genera including 5750 species having a worldwide distribution in the tropics and subtropics (Michelangeli et al., 2020). Members of this plant family are pioneer species and are thus important for habitat recovery in degraded areas. They are also heliophiles, that grow rapidly, are undemanding in terms of soil fertility, and their small fleshy fruits and

abundant seeds favour their establishment (Albuquerque et al., 2013; Arzolla et al., 2010; Jansen et al., 2002). Consequently, they are also commonly found in areas where *Eucalyptus* trees have been established in plantations and where their fungal pathogens potentially threaten plantation forestry (Granados et al., 2020; Gryzenhout et al., 2009; Oliveira et al., 2021; Rêgo et al., 2023; Silva et al., 2023; van der Merwe et al., 2013).

The genus *Chrysoporthe* is one of the most studied genera in the Cryphonectriaceae. Species cause typical canker symptoms, especially on Melastomataceae and Myrtaceae in tropical and subtropical regions (Gryzenhout et al., 2009, van der Merwe et al., 2013). Numerous species are known to have undergone host shifts (Slippers et al., 2005) from native trees and woody shrubs to infect *Eucalyptus* species (Oliveira et al., 2021; van der Merwe et al., 2013; Wingfield et al., 2001).

Nine species of *Chrysoporthe* have been described including, *C. cubensis*, *C. deuterocubensis*, *C. hodgesiana*, *C zambiensis*, *C. syzygiicola*, *C. doradensis*, *C. inopina*, *C austroafricana*, and *C. puriensis*. The species in th genus are morphologically very similar; consequently DNA sequence data and phylogenetic analyses are necessary for their accurate identification (Chungu et al., 2009; Gryzenhout et al., 2004, 2006; Oliveira et al., 2021). Among these species, only *C. cubensis, C. doradensis*, and *C. puriensis* have been reported to occur on the Myrtaceae and Melastomataceae in Brazil (Chungu et al., 2009; Gryzenhout et al., 2005; Hodges et al., 1976; Oliveira et al., 2021; Soares et al., 2018; Wingfield, 2003).

The first species of *Chrysoporthe* reported in Brazil was *C. cubensis*, which at the time resided in the genus *Diaporthe* (Hodges et al., 1976; Wingfield, 2003). The fungus was shown to cause a serious canker disease on *Eucalyptus* in plantations, but it was also found to occur on native plants (Seixas et al.,2004). *Chrysoporthe cubensis* was initially reported from Cuba on *Eucalyptus* spp. (Bruner et al., 1917) and was later

found in several tropical and subtropical countries (Nakabonge et al., 2007; Rodas et al., 2005; van der Merwe et al., 2010; Wingfield et al., 2001). It was first reported in Brazil in the 1970's (Hodges et al., 1976) and has become one of the most important fungal pathogens in Brazilian *Eucalyptus* plantations. This has resulted in the establishment of forest pathology programmes and tree-breeding initiatives to produce disease tolerant *Eucalyptus* genotypes (Ferreira, 1989; Wingfield et al., 2008).

Chrysoporthe doradensis was first described from Ecuador, causing cankers on *E. grandis* and *E. deglupta* (Gryzenhout et al., 2005). Subsequently, in 2015, this species was found in Brazil infecting *Eucalyptus* spp. in the states of Maranhão and Minas Gerais and *Pleoroma granulosum* (= *Tibouchina granulosa*) in Minas Gerais (Soares et al., 2018). Symptoms of infection were typical of canker diseases and very similar to those caused by *C. cubensis* (Gryzenhout et al., 2005; Soares et al., 2018; Oliveira et. al., 2021, 2022).

Most recently, *C. puriensis* was described from Brazil where it was found causing cankers on *Pleroma* spp. (Melastomataceae) in the states of Minas Gerais, Bahia, and Rio de Janeiro. Infections by *C. puriensis* commonly lead to the death of host trees, and pathogenicity tests have shown that it is also able to cause a canker disease on *Eucalyptus* hybrids (Oliveira et al., 2021).

Recent reports of new *Chrysoporthe* species in Brazil, and other genera in the Cryphonectriaceae such as the one causing canker on *Caryocar brasiliense* (Caryocaraceae) trees (Ferreira et al., 2019) suggest a wide diversity of these fungi in Brazil and that they deserve research attention. This is especially true given Brazil's Tropical and subtropical climatic conditions that favour the biology of the Cryphonectriaceae (Gryzenhout et al., 2009).

During field research conducted in south-eastern Brazil, symptoms, and signs typical of those caused by Cryphonectriaceae were observed on *Miconia* spp. and *Rhynchanthera grandiflora* plants, that reside in the Melastomataceae. The aim of this study was to isolate and identify this fungus utilising phylogenetic and morphological analyses, as well as assess its pathogenicity.

2. Materials and methods

2.1. Cultures

Miconia ibaguensis, *M. theaezans* and *R. grandiflora* trees growing close to water courses in the states of Rio de Janeiro and Minas Gerais, showing symptoms of die-back were sampled. Fruiting structures typical of the Cryphonectriaceae were obvious on dying branches and single samples were taken from different trees. The samples were stored in paper bags, labelled, and transported to the Laboratory of Forest Pathology, Universidade Federal de Lavras, Brazil.

A single fruiting body producing conidia was removed from each sample and suspended in water. The suspensions of conidia were transferred to Petri dishes containing potato dextrose agar (PDA) (Merck, Darmstadt, Germany) medium supplemented with rifamycin (100 mg/L) (Medley, São Paulo, Brazil) and incubated at 28 °C for 24 hours until the conidia had germinated.

Single germinated conidia were transferred to fresh Petri dishes containing PDA and then incubated at 28 °C for seven days to obtain pure cultures for storage. The isolate TILU 103 was deposited in the "Coleção de Culturas de Microorganismos" (CCDCA) at the Universidade Federal de Lavras and other isolates were stored in tubes containing sterilized water (Castellani, 1939) and kept at room temperature in the Laboratory of Forest Pathology. In addition, samples of branches from which isolate

TILU 103 was made, were deposited in the "Coleção Micológica do Herbário UB", Universidade de Brasília, Brazil.

2.2. DNA extraction, amplification, and sequencing

The mycelium used for DNA extraction was obtained following the methods described by Myburg et al. (1999). Mycelial discs 5 mm in diameter were transferred to Erlenmeyer flasks with liquid culture medium containing malt extract (20 g/L), yeast extract (2 g/L), and dextrose (5 g/L). The flasks were incubated for 7 days at 28°C allowing the fungus to grow. The mycelium was removed, filtered, dried on filter paper and then pulverised in liquid nitrogen.

DNA was extracted following the cationic hexadecyl trimethyl ammonium bromide (CTAB) method (Doyle and Doyle, 1987). For cell lysis, an extraction buffer containing Tris-Cl, EDTA, NaCl, and CTAB was used. The quality and concentration of the extracted fungal DNA was evaluated using agarose gel electrophoresis, visualized in ultraviolet-light image using a UV transilluminator (Mini BIS Pro, DNR Bio Imaging Systems, Jerusalem, Israel) and Nanodrop (Thermo Scientific NanoDrop 2000c Spectrophotometer), respectively.

Polymerase chain reactions (PCRs) were performed as described by Glass and Donaldson (1995). Each PCR had a final volume of 25 µL and was run on a Techne Prime G thermal cycler. Subsequently, the ITS region of the rDNA gene (ITS1-5.8S-ITS2), targeted by the primer pair ITS1 and ITS4, (White et al., 1990) and the BT1 and BT2 fragments of the β-tubulin gene, targeted by the primer pairs BT1a/BT1b and BT2a/BT2b, respectively (Glass and Donaldson, 1995) were amplified. PCR conditions were adjusted for each gene region. For the ITS region and BT1 fragment of the β-tubulin gene, the cycling conditions included denaturation at 94 °C for 1 minute,

150 followed by 35 cycles at 94 °C for 30 seconds, 55 °C for 55 seconds, and 72 °C for 2
151 minutes, with a final extension of 72 °C for 5 minutes. For the BT2 fragment, the
152 cycling conditions were denaturation at 94 °C for 1 minute; 35 cycles at 94 °C for 30
153 seconds, 62 °C for 45 seconds and 72 °C for 1 minute; and a final extension at 72 °C for
154 5 minutes. The amplification products were evaluated by electrophoresis in 1% agarose
155 gel with the addition of GelRed®. The bands were visualized using a UV
156 transilluminator (Mini BIS Pro, DNR Bio Imaging Systems, Jerusalem, Israel).
157 Purification of the PCR product and sequencing were performed by Macrogen (S.
158 Korea).
159
160 *2.3. Phylogenetic analyses*
161 The electropherograms resulting from Sanger sequencing were analysed, and the
162 sequences were manually edited, when necessary, using SeqAssem software (Hepperle,
163 2004). After editing, the sequences generated in this study were aligned with other
164 *Chrysoporthe* sequences available in GenBank database (Table 1). All sequences
165 generated in this study were submitted to NCBI/Genbank.
166 Multiple alignments of the sequences were performed using the online interface
167 of MAFFT version 7 software (Katoh et al., 2019) with the option L-INS-I. To
168 determine whether a combined analysis of the ITS and β-tubulin sequences was
169 acceptable, a partition homogeneity test was applied (Farris et al., 1995) using the
170 software PAUP* 4.0 (Swofford, 2002) Phylogenetic analyses were performed using the
171 maximum likelihood, maximum parsimony, and Bayesian inference methods.
172 The maximum likelihood analysis was done using MEGA software version 6.0
173 (Tamura et al., 2013). For the combined tree of the ITS, BT1, and BT2 regions, the
174 three-parameter Tamura evolutionary model was applied, as determined by MEGA

175 (Tamura, 1992) and the discrete gamma distribution was used to model the rate
176 variation among sites. The branch support was determined through 1000 bootstrap
177 replicates. All characters were included in the analysis. The Nearest-Neighbor-
178 Interchange (NNI) heuristic method was chosen, including a strong branch swap filter.

179 Maximum parsimony analysis was performed in PAUP* 4.0 (Swofford, 2002)
180 using only parsimony-informative characters. The analysis consisted of 100 replicates,
181 using the random addition of sequences and subsequent tree bisection and reconnection
182 branch swapping. The branch support values were estimated using 1000 bootstrap
183 replicates. The number of parsimony-informative characters, consistency index,
184 retention index, and rescaled consistency index were also calculated (Farris, 1989;
185 Kluge and Farris, 1969).

186 Bayesian inference was performed using MrBayes software, version 3.2.1
187 (Ronquist et al., 2012). The best-fit models were selected for AIC in MrModeltest and
188 GTR + G was applied to β-tubulin and K80+I for ITS. Branch support was indicated by
189 the posterior probability values (Huelsenbeck et al., 2001). The Markov chain Monte
190 Carlo algorithm (Larget and Simon, 1999) was generated from a random tree and
191 executed with 10^7 generations. A total of 25% of the initial samples collected were
192 discarded (burn-in), and the remaining samples were used to calculate the posterior
193 probability values. Sequences of *Amphilogia gyrosa* were used as outgroups in all
194 analyses, and the trees were analysed and edited in FigTree version 1.3.1
195 (http://tree.bio.ac.uk/software).
196
197 *2.4. Morphological characterization*

198 For morphological characterization of the species, longitudinal sections of the
199 fungal structures were made and mounted on glass slides. The size, shape, and colour of

200 the pycnidia, loculi, conidiophores and conidia were evaluated. Measurements were
201 performed for 50 replicates of each structure under a microscope (Nikon Eclipse E200,
202 Minato, Tokyo, Japan), equipped with an Infinity camera (Lumenera, Canada). Fungal
203 structures formed in culture were also observed under a Nikon SMZ 1500 stereoscopic
204 microscope (Nikon, Tokyo, Japan).

205 For detailed observation of conidia and conidiophores, scanning electron
206 microscopy (SEM) was used. For this purpose, the fruiting bodies and spore masses of
207 the fungus were collected from bark samples and fixed in Karnovsky solution (2.5%
208 glutaraldehyde, 2.5% paraformaldehyde in cacodylate buffer pH 7.2) in microtubes for
209 24 hours at 4 °C. The suspension was centrifuged, the excess supernatant reduced, and
210 the remaining suspension was transferred to coverslips treated with poly-L-lysine to
211 facilitate adhesion of the material.

212 After 10 minutes, the material was post- fixed in 1% osmium tetroxide (OsO_4)
213 and washed in 0.05 M cacodylate buffer three times for 10 minutes. The samples were
214 then dehydrated in graded acetone solutions at concentrations of 25, 50, 75, 90, and
215 100%. After dehydration of the samples on a critical point dryer (BAL-TEC, CPD-030),
216 the coverslips containing the structures were adhered to stubs and gold-coated in an
217 SCD 050 Bal-Tec sputter coater After these treatments, the samples were viewed using
218 an LEO EVO 40XVP (Cambridge, UK) scanning electron microscope.

219

220 *2.5. Pathogenicity tests*

221 To test whether the *Chrysoporthe* sp. considered in this study was pathogenic,
222 artificial inoculations were made. Two different methods were used. These included *R.*
223 *grandiflora* seedlings as well as stem sections cut from healthy *R. grandiflora* and *M.*
224 *theaezans* plants.

225 Six seedlings of *R. grandiflora*, approximately one-year-old, were inoculated
226 with the *Chrysoporthe* sp. isolate TILU 103. Disks of bark (5mm diameter) were
227 removed from the stems of the plants to expose the cambium, using a cylindrical punch.
228 Subsequently, 5mm discs of mycelium taken from 7-day-old cultures on PDA were
229 placed in contact with the cambium and the inoculation sites were covered with plastic
230 film for 30 days to reduce contamination and to prevent desiccation of the inoculum.
231 Six plants were inoculated in the same manner, but with sterile PDA, serving as
232 controls. The experiment was conducted in a greenhouse maintained at temperatures
233 ranging from 15 to 27 °C and the results were recorded 60 days after inoculation.
234 For the inoculations using cut stem sections, ten stems each of *R. grandiflora*
235 and *M. theaezans*, approximately 10 mm in diameter, were inoculated using the same
236 methods used for the *R. grandiflora* seedlings. These experiments were conducted
237 entirely randomly, and the stem sections were maintained in a humid chamber at 25 °C.
238 The plastic film covering the inoculation wounds was retained throughout the
239 experiment and the results were evaluated after 21 days.
240 The experiments were repeated once, and lesion lengths on the seedling plants or
241 cut stems were measured to assess the pathogenicity. To compare the mean lesion
242 lengths of the control and inoculated plants a t-test was conducted using the software R
243 and values where $P \leq 0.05$ were considered as significant. After measuring lesion lengths,
244 isolations were made from lesions on three *R. grandiflora* seedlings and three each of
245 the excised *R. grandiflora* and *M. theaezans* stems to fulfil the Koch's postulates.
246
247 3. Results
248 *3.1. Isolates and symptoms*

A total of eight isolates (Table 1) were obtained, each of which was obtained from a different symptomatic tree. One isolate was obtained from a *M. ibaguensis* tree Itatiaia National Park, Rio de Janeiro (22°29′45″S and 44°39′39″W), four were from *R. grandiflora* trees in the city of Luminárias, Minas Gerais (21°19′44″S and 44°58′6″W) (Fig 1A) and three isolates were from *M. theaezans* trees in the Quedas do Rio Bonito Ecological Park, Lavras, Minas Gerais (21°19′44″S and 44°58′6″W), (Fig 1B).

The symptoms on the diseased trees were different for *Miconia* spp. and *R. grandiflora*. In the case of *Miconia*, there were slits in the bark on the tree trunks (Fig 1C), trees had many dry branches and there was severe defoliation, leading to partial tree death. In the case of *R. grandiflora,* the entire trees had died. Pycnidia of a fungus resembling those in the Cryphonectriaceae were common on the bark of the dead branches and stems of both hosts (Fig 1D).

3.2. Phylogenetic analyses

The amplicons obtained by PCR were approximately 437 bp for the ITS region and 685 bp for β-tubulin (336 bp for BT1 and 349 for BT2). The partition homogeneity test of the combined sequences was P = 0.01, indicating that the data sets were incongruent. Since this value was very low and other authors (Chen et al., 2010; Oliveira et al., 2021) have combined these data, a combined tree (Figure 2) was chosen for presentation and the individual trees are included as Supplementary Data (Figure 1S and 2S).

The trees generated based on maximum likelihood (ML), maximum parsimony (MP), and Bayesian inference (BI) analyses showed the same topology with well-supported branches having high bootstrap and posterior probability values.

The alignment of the combined BT2, BT1 and ITS sequences had a total of 1,122 characters, of which 1000 were constant, ten were non informative, and 112 were informative. The values obtained were 0.78 for the consistency index, 0.21 for homoplasy index, 0.87 for the retention index, and 0.68 for the rescaled consistency index.

In all analyses, the *Chrysoporthe* spp. sequences grouped into nine well-supported clades (more than 70% bootstrap and 0.9 posterior probability). The eight isolates resulting from this study grouped in a distinct clade with high support values (ML/MP/BI: 99/100/1.0). This supported the conclusion that the *Chrysoporthe* species had not previously been described. The alignment of the β-tubulin and ITS sequences of all *Chrysoporthe* species showed that the difference between them was due to the presence of 53 polymorphic nucleotides, of which nine were autoapomorphic for the undescribed species (Table 2).

3.3. Taxonomy and morphology

Analysis of the DNA sequences showed that the isolates collected in the present study were of an undescribed *Chrysoporthe* species. Morphologically, the characteristics were similar to those of other *Chrysoporthe* spp. (Table 3), but with subtle differences, such as smaller conidiomata, conidiophores, and conidia. The new species is thus described as follows:

Chrysoporthe brasiliensis G.A. Sil., M.E.S. Oliv., & M.A. Ferr**., sp. nov.**

Mycobank:

Etymology: The name "*brasiliensis*" refers to the fact that the fungus was found in Brazil.

298 *Ascostromata:* not observed.

299 *Conidiomata:* Pycnidia superficial to semi-immersed in the bark of branches and
300 trunks of the host. Matt black in colour, mostly pulvinate, conical or pyriform, with
301 bases 57-(206.5)-372 µm, and single ostiolate necks 75.2-(205.0)-354.1 µm. Most
302 pycnidia with a single locule, or rarely two, convoluted, with 27.5-(104.0)-212.5 µm
303 long and 23.5-(87.5)-170.5 µm (Fig 3A), wide stromal tissue golden-brown with a
304 globular texture closer to the base and an epidermoid texture close to the conidiogenous
305 cells. Conidiophores hyaline, with globular to rectangular basal cells and 6.0-(9.5)-12.0
306 µm long, paraphyses 24.3-(34.6)-48.1 µm long, occasionally present between the
307 conidiophores (Fig 3B). Conidiogenous cell hyaline, cylindrical with attenuated apices,
308 3.5-(5.5)-7.5 µm (Fig 3C) with phialidic conidiogenesis. Conidia aseptate, hyaline, and
309 oblong, cylindrical, fusoid, oval, or ellipsoid (Fig 3D), 0.5-(1.0)-1.5 µm wide and 2.0-
310 (2.5)-4.5 µm long.

311 *Culture characteristics:* Colonies on PDA medium with a fluffy white growth
312 and becoming brownish-orange with age. Growth at 25 to 30 °C. At this temperature,
313 some cultures incubated for approximately 30 days produced pycnidia with yellow-
314 orange conidial masses (Fig 3E-F).

315 *Substrate:* Bark of branches and trunks of *Miconia ibaguensis*, *Miconia*
316 *theaezans* and *Rhynchanthera grandiflora*

317 *Distribution:* southeast Brazil: Minas Gerais and Rio de Janeiro States.

318 *Material examined:* Brazil, Minas Gerais State, Luminárias, *Rhynchanthera*
319 *grandiflora,* collected in 2018, MA Ferreira, Holotype TILU 103 = UB24348 (branches
320 with mature pycnidia), Ex-type culture TILU 103 = CCDCA11647

321 *Other specimens examined:* MIPNI01, Brazil, Rio de Janeiro State, Itatiaia
322 National Park (22°29′45″S and 44°39′39″W), *M. ibaguensis*, MES Oliveira and MA

323 Ferreira. MIL06, MIL 104B and MILS01E, Brazil, Minas Gerais State, Lavras, Quedas
324 do Rio Bonito Ecological Park (21°19′44″S and 44°58′6″W), *M. theaezans*, collected in
325 2018 by GA Silva, MES Oliveira, and MA Ferreira. TILU104, TILU 104D and TILU
326 308, Brazil, Minas Gerais State, Luminárias (21°19′44″S and 44°58′6″W), *R.*
327 *grandiflora*, MA Ferreira, and GA Silva.

328 *Notes: Chrysoporthe brasiliensis* isolates grouped in a clade distinct from all
329 other species in this genus with high bootstrap and posterior probability support. Like
330 other species in the genus, it has superficial to semi-immersed conidiomata having a
331 matt-black colour. *Chrysoporthe brasiliensis* has smaller conidiophores and
332 conidiomata than other *Chrysoporth*e spp. (Table 3). Similar to *C. puriensis*, its
333 conidiomata occasionally have paraphyses (Oliveira et al., 2021), which have not been
334 found in other *Chrysoporthe* species.

335

336 *3.4. Pathogenicity*

337 Necrotic lesions were observed in all *R. grandiflora* seedling plants inoculated
338 with *C. brasiliensis*. This was in contrast to the control inoculations that were free of
339 any signs of infection (Fig. 4.A-D). A t-test revealed significant differences among
340 lesion sizes on the inoculated (72– 90.83 – 108 mm) and control plants (8 – 15.8 – 27
341 mm) ($P \leq 0.05$) (Fig. 4E).

342 The *R. grandiflora* and *M. theaezans* stem sections inoculated with *C.*
343 *brasiliensis* had dark-coloured lesions (Fig. 4B and D), which were not observed in the
344 control treatments (Fig. 4A and C). The t-test showed significant differences between *R.*
345 *grandiflora* stems inoculated (100 mm) and controls (1 – 3,92 -6 mm) and *M. theaezans*
346 stems inoculated (70 – 85.2 – 100 mm) and the controls (1 – 4.44 – 9 mm) ($P \leq 0.05$)
347 (Fig. 4E).

348 The inoculated fungus could be re-isolated from inoculated seedlings and stems,
349 but not from controls, thus fulfilling Koch's postulates. It was possible to detect the
350 presence of pycnidia on the bark of *R. grandiflora* plants 90 days after inoculation.
351
352 **4. Discussion**
353 This study resulted in the discovery of a new species of *Chrysoporthe*, described
354 here as *C. brasiliensis,* which is pathogenic on two native genera of the
355 Melastomataceae in southeast Brazil. This is the fourth species of *Chrysoporthe* to be
356 discovered on species of the Myrtales in Brazil (Oliveira et al., 2021, 2022; Soares et
357 al., 2018; Rêgo et al., 2023; Silva et al., 2023). The results suggest that this is a group of
358 fungi that remain relatively unexplored in the area.
359 The symptoms on *Miconia* spp. and *R. grandiflora* plants infected by *C.*
360 *brasiliensis* were similar to those associated with other species of *Chrysoporthe*. This is
361 clearly an aggressive species with the potential to cause severe damage where
362 conditions favour its establishment. Of particular concern is whether the fungus would
363 be able to infect commercially propagated trees such as *Eucalyptus,* which are widely
364 planted in Brazil to sustain large and important forest enterprises. In this regard, the
365 closely related *C. cubensis* has caused substantial damage to Brazilian *Eucalyptus*
366 plantations in the past and is known to have stimulated the first efforts to produce these
367 trees through vegetative propagation (Ferreira, 1989; Gryzenhout et al., 2009; Wingfield
368 et al., 2008;). Determining the pathogenicity of *C. brasiliensis* on commercially
369 propagated *Eucalyptus* genotypes should be a priority for future research.
370 Tree pathogens in the Cryphonectriaceae are apparently rising in importance.
371 This view is based on the fact that there are increasing numbers of fungi in this family
372 being discovered, specifically species of *Chrysoporthe.* Many of these have the ability

to undergo host shifts to infect non-native and commercially important trees such as *Eucalyptus* (van der Merwe et al., 2013). These pathogens, for example, include *C. cubensis*, *C. deuterocubensis*, *C. austroafricana*, *C. doradensis* and *C. puriensis*, all of which occur on the Melastomataceae but can infect *Eucalyptus.*

The origin of *C. brasiliensis* is unknown, but its occurrence on native Brazilian Melastomataceae suggests that it is native to the area where it was discovered. This is an important question that needs to be investigated to understand its potential threat to trees in the Myrtales elsewhere in the world. Population genetic studies such as those that have been conducted on *C. cubensis*, *C. puriensis*, *C. deuterocubensis*, and C. *austroafricana* have shown that these fungi are moving between their native and planted hosts (Granados et al., 2020; Heath et al., 2006; van der Merwe et al., 2013). As these diseases increase in number, it is possible, perhaps even probable, that they could be accidentally introduced into new environments where they would threaten native woody species. This would be analogous to better-studied diseases such as chestnut blight, Dutch elm disease and white pine blister rust where the causal pathogens have moved between northern hemisphere countries (Sinclair and Lyon, 2005), but in this case across the southern hemisphere.

5. Conclusions

Results of this study led to the identification of a new species *of Chrysoporthe*, *C. brasiliensis*, causing a serious disease on trees in the Melastomataceae. The fungus was recognised as a novel taxon mainly using DNA sequence-based phylogenetic inference and supported by morphological characteristics. Inoculation trials showed that *C. brasiliensis* was pathogenic to *R. grandiflora* and *M. theaezans*; the hosts on which it

was found. Based on previous studies on *Chrysoporthe* spp., *C. brasiliensis* may represent a threat to commercially propagated *Eucalyptus* in Brazil.

6. Acknowledgments

We are grateful to staff of the Electron Microscopy and Ultrastructural Analysis Laboratory and the Laboratory of Plant Anatomy - Universidade Federal de Lavras for support. Professor Olinto Liparini Pereira and Fábio Alex Custódio provided assistance with microscopy and image capture, and Mariana Mansanares, Maria Tereza Costa, Diego Nunes and Iago Augusto assisted us in identifying the Melastomataceae species. We also appreciate the ICMBio and Parque Ecológico Quedas do Rio Bonito that provided authorisation to collect samples The first author thanks the Conselho Nacional de Desenvolvimento Científico e Tecnológico (CNPq), FAPEMIG and the Coordenação de Aperfeiçoamento de Pessoal de Nível Superior (CAPES) for financial support via a scholarship..

7. References

Albuquerque, L.B., Aquino, F.G., Costa, L.C., Miranda, Z.J.G., Sousa, S.R., 2013. Espécies de Melastomataceae juss. com potencial para restauração ecológica de mata ripária no Cerrado. Polibotánica. 35, 1-19.

Anagnostakis, S.L., 1987. Chestnut Blight: The Classical Problem of an Introduced Pathogen. Mycologia. 79, 23-37.

420 Arzolla, F.A.R.D.P., Vilela, F.E.S.P., Paula, G.C.R. de, Shepherd, G.J., 2010.
421 Regeneração natural em clareiras de origem antrópica na Serra da Cantareira - SP.
422 Revis. Inst. Florestal. 22, 155-169.
423
424 Bruner, S.C., 1917. Una enfermedad gangrenosa de lós eucaliptos. Estaciòn
425 Experimental Agronòmica, Santiago de las Vegas, Cuba, Bulletin. 37, 1-33.
426
427 Castellani, A., 1939. Viability of some pathogenic fungi in distilled water. Am. J. Trop.
428 Med. Hyg. 42, 225-226.
429
430 Chen, S., Gryzenhout, M., Roux, J., Xie, Y., Wingfield, M. J., Zhou, X. D., 2010.
431 Identification and pathogenicity of *Chrysoporthe cubensis* on *Eucalyptus* and
432 *Syzygium* spp. in South China. Plant Dis. 94, 1143-1150.
433
434 Chungu, D., Gryzenhout, M., Muimba-Kankolongo, A., Wingfield, M.J., Roux, J.,
435 2009. Taxonomy and pathogenicity of two novel *Chrysoporthe* species from
436 *Eucalyptus grandis* and *Syzygium guineense* in Zambia. Mycol. Prog. 9, 379–393.
437
438 Crous, P.W., Summerell, B.A., Alfenas, A.C.; Edwards, J., Pascoe, I.G., Porter, I.J.,
439 Groenewald, J.Z., 2012. Genera of diaporthalean coelomycetes associated with leaf
440 spots of tree hosts. Persoonia. 28, 66-75.
441
442 Doyle, J.J., Doyle, J.L., 1987. A rapid DNA isolation procedure for small quantities of
443 fresh leaf tissue. Phytochemical Bulletin. 19, 11-15.
444

445 Fairchild, D., 1913. The discovery of the chestnut bark disease in China. Science. 38,
446 297-299.
447
448 Farris, J.S., 1989. The retention index and the rescaled consistency index. Cladistics. 5,
449 417–419.
450
451 Farris, J.S., Kallersjo, M., Kluge, A.G., Bult, C., 1995. Testing significance of
452 incongruence. Cladistics. 10, 315–319.
453
454 Ferreira, F.A., 1989. Patologia florestal: principais doenças florestais no Brasil.
455 Sociedade de Investigações Florestais: Viçosa, Brasil, 570p.
456
457 Ferreira, M.A., Oliveira, M.E.S., Silva, G.A., Mathioni, S.A., Mafia, R.G., 2019.
458 *Capillaureum caryovora* gen. sp. nov. (Cryphonectriaceae) pathogenic to pequi
459 (*Caryocar brasiliense*) in Brazil. Mycol. Prog. 18, 385-403.
460
461 Glass, N.L., Donaldson, G.C., 1995. Development of primer sets designed for use with
462 the PCR to amplify conserved genes from filamentous ascomycetes. Appl. Environ.
463 Microbiol. 61, 1323-1330.
464
465 Granados, M.G., MC Taggart, A.R., Rodas, C.A., Roux, J., Wingfield, M.J., 2020.
466 Species of Cryphonectriaceae occupy an endophytic niche in the Melastomataceae
467 and are putative latente pathogens of *Eucalyptus*. Plant Pathol. 156, 273-283.
468

469 Gryzenhout, M., Myburg, H., van der Merwe, N.A., Wingfield, B.D., Wingfield, M.J.,
470 2004. *Chrysoporthe*, a new genus to accommodate *Cryphonectria cubensis*. Stud.
471 Mycol. 50, 119–142.
472
473 Gryzenhout, M., Myburg, H., Wingfield, B.D., Montenegro, F., Wingfield, M.J., 2005.
474 *Chrysoporthe doradensis* sp. nov. pathogenic to *Eucalyptus* in Ecuador. Fungal
475 Divers. 20, 39-57.
476
477 Gryzenhout, M., Rodas, C.A., Portales, J.M., Clegg, P., Wingfield, B.D., Wingfield,
478 M.J., 2006. Novel hosts of the *Eucalyptus* canker pathogen *Chrysoporthe cubensis*
479 and a new *Chrysoporthe* species from Colombia. Mycological Research. 110, 833-
480 845.
481
482 Gryzenhout, M., Wingfield, B.D., Wingfield, M.J., 2009. Taxonomy, Phylogeny, and
483 Ecology of Bark-infecting and Tree Killing Fungi in the Cryphonectriaceae. APS
484 Press. 119p.
485
486 Gryzenhout, M., Tarigan, M., Clegg, P.A., Wingfield, M.J., 2010. *Cryptometrion*
487 *aestuescens* gen. sp. nov. (Cryphonectriaceae) pathogenic to *Eucalyptus* in Indonesia.
488 Austral. Plant Pathol. 39, 161-169.
489
490 Heath, R.N., Gryzenhout, M., Roux, J., Wingfield, M.J., 2006. Discovery of the canker
491 pathogen *Chrysoporthe austroafricana* on native *Syzygium* spp. in South Africa.
492 Plant Dis. 90, 433-438.
493

494 Hepperle, D., 2004. SeqAssem©: Win32-Version. A sequence analysis tool contig
495 assembler and trace data visualization tool for molecular sequences.
496 http://www.sequentix.de .
497
498 Hodges, C.S., Reis, M.S., Ferreira, F.A., Henfling, J.D.M., 1976. O cancro do eucalipto
499 causado por *Diaporthe cubensis*. Fitopatalogia Brasileira. 1, 129-170.
500
501 Huelsenbeck, J.P., Ronquist, F., 2001. MRBAYES: Bayesian inference of phylogenetic
502 trees. Bioinformatics. 17, 754–755.
503
504 Jansen, S., Watanabe, T., Smets, E., 2002. Aluminium accumulation in leaves of 127
505 species in Melastomataceae, with comments on the order Myrtales. Ann. Bot. 90, 53-
506 64.
507
508 Katoh, K, Rozewick, J, Yamada, K.D., 2019. MAFFT online service: multiple sequence
509 alignment, interactive sequence choice and visualization. Brief. Bioinform. 20, 1160-
510 1166.
511
512 Kluge, A., Farris, J.S., 1969. Quantitative phyletics and the evolution of anurans.
513 Systematic Zoology. 18, 1-32.
514
515 Larget, B., Simon, D.L., 1999. Markov chain Monte Carlo algorithms for the Bayesian
516 analysis of phylogenetic trees. Mol. Biol. Evol. 16, 750–759.
517

518 Michelangeli, F., Almeda, F., Goldenberg, R., Penneys, D., 2020. A Guide to Curating
519 New World Melastomataceae Collections with a Linear Generic Sequence to World-
520 Wide Melastomataceae. Preprints. Published on the Internet. http://www.preprints.
521 org.
522
523 Myburg, H., Wingfield, B.D., Wingfield, M.J., 1999. Phylogeny of *Cryphonectria*
524 *cubensis* and allied species inferred from DNA analysis. Mycologia. 91, 243-250.
525
526 Nakabonge, G., Gryzenhout, M., Wingfield, B. D., Wingfield, M. J., Roux, J., 2007.
527 Genetic diversity of *Chrysoporthe cubensis* in eastern and southern Africa. S. Afr. J.
528 Sci. 103, 261-264.
529
530 Oliveira, M.E.S., Kanzi, A.M., van der Merwe, N.A., Wingfield, M.J., Wingfield, B.D.,
531 Silva, G.A., Ferreira, M.A., 2022. Genetic variability in populations of *Chrysoporthe*
532 *cubensis* and *Chr. Puriensis* in Brazil. Austral. Plant Pathol. 51, 175–191.
533
534 Oliveira, M.E.S., van der Merwe, N.A., Wingfield, M.J., Wingfield, B.D., Soares,
535 T.P.F., Kanzi, A.M., Ferreira, M.A., 2021. *Chrysoporthe puriensis* sp. nov. from
536 *Tibouchina* spp. in Brazil: an emerging threat to *Eucalyptus*. Austral. Plant Pathol.
537 50, 29-40.
538
539 Rêgo, G.M.S., Souza, I.A.L., Silva, G.A., Oliveira, M.E.S., Ferreira, M. A., 2023.
540 *Chrysoporthe puriensis* causing canker and mortality in *Pleroma mutabile* in the
541 Atlantic Forest, Brazil. For. Pathol. 53, e12803.
542

543 Rodas, C.A., Gryzenhout, M., Myburg, H., Wingfield, B.D., Wingfield, M.J., 2005.
544 Discovery of the *Eucalyptus* canker pathogen *Chrysoporthe cubensis* on native
545 *Miconia* (Melastomataceae) in Colombia. Plant Pathol. 54, 460–470.
546
547 Ronquist, F., Teslenko, M., van der Mark, P., Ayres, D.L., Darling, A., Höhna, S.,
548 Larget, B., Liu, L., Suchard, M.A., Huelsenbeck, J.P., 2012. MrBayes 3.2: efficient
549 Bayesian phylogenetic inference and model choice across a large model space. Syst.
550 Biol. 61, 539–542.
551
552 Seixas, C.D.S., Barreto, R.W., Alfenas, A.C., Ferreira, F.A., 2004. *Cryphonectria*
553 *cubensis* on an indigenous host in Brazil: a possible origin for eucalyptus canker
554 disease? Mycologist. 18, 39-45.
555
556 Silva, G.A.; Moreira, S.I.; Ferreira, M.A., 2023. New Melastomataceae hosts of
557 *Chrysoporthe* species in Brazil. J. Phytopathol. 0, 1-7.
558
559 Sinclair, W.A.; Lyon., H.H. Diseases of trees and shrubs, 2005. No. Ed. 2. Comstock
560 Publishing Associates.
561
562 Slippers, B., Stenlid, J., Wingfield, M.J., 2005. Emerging pathogens: fungal host jumps
563 following anthropogenic introduction. Trends Ecol. Evol. 20, 420–421.
564
565 Soares, T.P.F., Ferreira, M.A., Mafia, R.G., Oliveira, L.S.S., Hodges, C.S., Alfenas,
566 A.C., 2018. Canker disease caused by *Chrysoporthe doradensis* and *C. cubensis* on
567 *Eucalyptus* sp. and *Tibouchina* spp. in Brazil. Trop. Plant Pathol. 43, 314–322.

Swofford, D.L. PAUP* phylogenetic analyzes using Parsimony: and other methods. Version 4.0 beta. http://paup. csit. fsu./ 2002.

Tamura, K., 1992. Estimation of the number of nucleotide substitutions when there are strong transition-transversion and G + C-content biases. Mol. Biol. Evol. 9, 678-687.

Tamura, K., Stecher, G., Peterson D., Filipski, A., Kumar, S., 2013. MEGA6: molecular evolutionary genetics analysis version 6.0. Mol. Biol. Evol. 30, 2725–2729.

van der Merwe, N.A., Gryzenhout, M., Steenkamp, E.T., Wingfield, B.D., Wingfield, M.J., 2010. Multigene phylogenetic and population differentiation data confirm the existence of a cryptic species within *Chrysoporthe cubensis.* Fungal Biol. 114, 966-979.

van der Merwe, N.A., Steenkamp, E.T., Rodas, C., Wingfield, B.D., Wingfield, M.J., 2013. Host switching between native and non-native trees in a population of the canker pathogen Chrysoporthe cubensis from Colombia. Plant Pathol. 62, 642–648.

Wang, W., Liu, Q.L., Li, G.Q., Liu, F., Chen, S.F., 2018. Phylogeny and pathogenicity of *Celoporthe* species from plantation *Eucalyptus* in Southern China. Plant Dis. 102, 1915-1927.

Wang, W., Li, G.Q., Liu, Q.L., Chen, S.F., 2020. Cryphonectriaceae on Myrtales in China: phylogeny, host range, and pathogenicity. Persoonia. 45, 101–131.

White, T.J., Bruns, T., Lee, S.J.W.T., Taylor, J., 1990. Amplification and direct sequencing of fungal ribosomal RNA genes for phylogenetics. PCR protocols: a guide to methods and applications. 18, 315-322.

Wingfield, M.J., Rodas, C., Myburg, H., Venter, M., Right, J., Wingfield, B.D., 2001. *Cryphonectria* canker on *Tibouchina* in Colombia. Forest Pathol. 31, 297–523.

Wingfield, M.J., 2003. Daniel McAlpine Memorial Lecture. Increasing threat of diseases to exotic plantation forests in the Southern Hemisphere: lessons from Cryphonectria canker. Austral. Plant Pathol. 23, 133–139.

Wingfield, M..J., Slippers, B., Hurley, B.P., Coutinho, T.A., Wingfield, B.D., Roux, J., 2008. Eucalypt pests and diseases: growing threats to plantation productivity. South. Forests: a Journal of Forest Science. 70, 139-144.

Abbreviations: ITS= internal transcribed spacer BT1= β-tubulin gene region 1. BT2= β-tubulin gene region 2. PDA= potato dextrose agar medium.

Sequences of Holotype TILU 103

>TILU103 ITS

CCTTTTTATCGTTGCCTCGGCGCCGAGCCGGGAGTGCTCTTTTGTGCTCCCCC
ACCGCGTAAGCAGTGGAGCAGGCCCGCCGGCGGCCCACCAAACTCTTTGTT
TTTAGAACGTATCTCTTTCTGAGTGTTTATAACAAACAAATGAATCAAAACT
TTCAACAACGGATCTCTTGGTTCTGGCATCGATGAAGAACGCAGCGAAATG

CGATAAGTAATGTGAATTGCAGAATTCAGTGAATCATCGAATCTTTGAACG

CACATTGCGCCCGCTGGAATTCCAGCGGGCATGCCTGTTCGAGCGTCATTTC

AACCCTCAAGCCTGGCTTGGTGTTGGGGCACTACCTGTTCACAGCGGGTAG

GCCCTGAAATTTAGTGGCAGGCTCGCTAAGACTCTGAGCGTAGTAGTTTTTA

TCACCTCGCTTTGGAAGG

>TILU103 BT1

GACCCCAAGAACATGATGGCTGCCTCTGACTTCCGCAACGGTCGCTACCTG

ACGTGCTCCGCCATCTTGTAAGTCCCCCGCCCCTCGCCCCTCGGGGAGCATC

GGCCGAAGCTTGGCTGCTAACCCTCATCGTTCGTCCAGCCGTGGCAAGGTCT

CCATGAAGGAGGTCGAGGATCAGATGCGCAACGTCCAGAGCAAGAACTCGT

CCTACTTCGTCGAGTGGATCCCCAACAACGTCCAGACCGCCCTCTGCTCCAT

CCCCCCCAAGGGTCTCAAGATGTCCTCCACCTTTGTTGGCAACTCCACTGCC

ATCCAGGAGCTCTTCAAGCGTATCGGCGAGCAGTTCACT

>TILU103 BT2

CAAACCATCTCTGGCGAGCACGGCCTCGACAGCAATGGCGTGTACGTACCC

TCCTGCTGCACCAGGCGGCGCGCCTCGAGCTTCTCGCTGACCACCGCACAGC

TACAACGGCACCTCCGAGCTCCAGCTCGAGCGCATGAACGTCTACTTTAAC

GAGGTATGTCTGTCGGGACCAGGCTGGGGCGTCATCCCGCCCGCGTACCCC

CTGTGCGTGACCGAGCTCCCGCTGACGCGCTCCTGTCACAGGCCTCCGGCAA

CAAGTATGTTCCCCGCGCCGTCCTCGTCGATCTCGAGCCCGGCACCATGGAC

GCC

643 **Table 1** *Chrysoporthe* spp. and *Amphilogia gyrosa* (outgroup) reference sequences used

644 in the present study.

Species	Isolate number	Host/substrate	Location	GenBank accession number		
				ITS	BT1	BT2
Chrysoporthe brasiliensis	**MIL06**	*Miconia theaezans*	Minas Gerais - Brazil	MT886851	OP714218*	
	MIL104B	*Miconia theaezans*	Minas Gerais - Brazil	MT886850	OP714219*	
	MILS01E	*Miconia theaezans*	Minas Gerais - Brazil	ON000431	OP714220*	
	MIPNI01	*Miconia ibaguensis*	Rio de Janeiro - Brazil	MT886852	OP714221*	
	TILU103	*Rhynchanthera grandiflora*	Minas Gerais - Brazil	MT886849	OP714222*	
	TILU104	*Rhynchanthera grandiflora*	Minas Gerais - Brazil	MT886848	OP714223*	
	TILU104D	*Rhynchanthera grandiflora*	Minas Gerais - Brazil		OP714224*	
	TILU308	*Rhynchanthera grandiflora*	Minas Gerais - Brazil	ON000430	OP714225*	
Chrysoporthe doradensis	CMW11286	*Eucalyptus grandis*	Ecuador	AY214290	AY214218	AY214254
	CMW11287	*Eucalyptus grandis*	Ecuador	GQ290156	GQ290179	GQ290190
Chrysoporthe inopina	CMW12729	*Pleroma lepidotum*	Colombia	DQ368778	AH015656*	
	CMW12727	*Pleroma lepidotum*	Colombia	DQ368777	AH015657*	
Chrysoporthe hodgesiana	CMW10625	*Miconia theaezans*	Colombia	AY956970	AH014900*	
	CMW10641	*Pleroma semidecandrum*	Colombia	AY692322	AY692326	AY692325
Chrysoporthe deuterocubensis	CMW12745	*Pleroma urvilleanum*	Singapore	DQ368764	GQ290183	DQ368781
	CMW18515	*Melastoma malabathricum*	Indonesia	JN942341		

Chrysoporthe cubensis	CMW14394	*Eucalyptus grandis*	Cuba	DQ368773	AH015642*	
	CMW10639	*Eucalyptus grandis*	Colombia	AY263421	AY263419	AY263420
Chrysoporthe puriensis	CT13	*Pleroma granulosum*	Brazil	MN590029	MN590041*	
	TCL01	*Pleroma candolleanim*	Brazil	MN590030	MN590042*	
Chrysoporthe syzygiicola	CMW29940	*Syzygium guineense*	Zambia	FJ655005	FJ805230	FJ805236
	CMW29941	*Syzygium guineense*	Zambia	FJ655006	FJ805231	FJ805237
Chrysoporthe zambiensis	CMW29930	*Eucalyptus grandis*	Zambia	FJ655004	FJ858711	FJ805235
	CMW29928	*Eucalyptus grandis*	Zambia	FJ655002	FJ858709	FJ805233
Chrysoporthe austroafricana	CMW2113	*Eucalyptus grandis*	South Africa	AF046892	AF273067	AF273462
	CMW9327	*Pleroma granulosum*	South Africa	GQ290158	GQ290185	AF273455
Amphilogia gyrosa	CMW10469	*Ealeocarpus dentatus*	New Zealand	AF452111	AF525707	AF525714
	CMW10470	*Ealeocarpus dentatus*	New Zealand	AF452112	AF525708	AF525715

645 Isolates in bold were sequenced in this study.

646 CMW= Forestry and Agricultural Biotechnology Institute (FABI), University of

647 Pretoria.

648 *Sections of BT1/BT2 combined of the gene β-tubulin.

Table 2 Summary of polymorphic sites found in the ITS and β-tubulin gene sequences for the different *Chrysoporthe* species. Autapomorphies for *Chrysoporthe brasiliensis* are highlighted.

Species	Beta tubulin 2										Beta tubulin 1															ITS				
	27	66	85	95	97	145	201	289	298	319	411	413	424	425	431	432	446	467	471	511	574	577	601	628	727	749	1032	1069	
Chrysoporthe brasiliensis	C	G	**T**	C	G	C	**T**	T	C	**C**	C	C	C	**C**	G	G	A	**C**	C	**T**	C	G	C	T	**T**	**T**	A	C	**A**
Chrysoporthe doradensis	C	G	C	C	G	C	G	T	C	T	C	C	T	G	A	G	A	-	C	C	C	G	A	T	C	C	A	C	G
Chrysoporthe inopina	C	G	C	C	A	C	A	T	C	T	C	C	C	G	G	G	A	T	C	C	C	G	C	T	C	C	A	C	G
Chrysoporthe hodgesiana	C	A	C	C	G	C	A	C	C	T	C	C	C	G	G	G	G	-	C	C	C	G	C	T	C	C	A	C	G
Chrysoporthe deuterocubensis	C	G	C	C	G	C	A	T	T	T	C	C	C	G	G	G	A	-	C	C	C	G	C	T	C	C	G	C	G
Chrysoporthe cubensis	C	G	C	C	G	C	A	T	C	T	C	C	C	G	G	A	A	-	C	C	C	G	C	T	C	C	A	C	G
Chrysoporthe puriensis	T	G	C	T	G	C	A	T	C	T	T	T	C	G	G	G	A	-	T	C	C	G	C	T	C	C	A	C	G
Chrysoporthe syzygiicola	C	G	C	C	G	C	A	T	C	T	C	C	C	G	G	G	A	-	C	C	A	T	C	T	C	C	A	C	G
Chrysoporthe zambiensis	C	G	C	C	G	A	A	T	C	T	C	C	C	G	G	G	A	-	C	C	C	G	C	A	C	C	A	A	G
Chrysoporthe austroafricana	C	G	C	C	G	C	A	T	C	T	C	C	C	G	G	G	A	-	C	C	C	G	C	T	C	C	A	C	G

652 **Table 3** Comparison of morphological characteristics of *Chrysoporthe* spp.

Species	Conidiomata		Conidial locules	Conidium			Conidiogenous cell length(µm)	Paraphyses	References
	Shape	Base width (µm)		Shape	Length(µm)	Width(µm)			
Chrysoporthe brasiliensis	Pulvinate to conic, pyriform	57-372	unilocular or multilocular	oblong, fusoid, cylindrical, oval	2.0-4.5	0.5-1.5	6.0-12.0	Present	This study
Chrysoporthe doradensis	Pyriform to pulvinate	100-290	multilocular	oblong, oval, cylindrical, alantoid	3-6.5	1.5-2.5	9.5-21.5	Absent	Gryzenhout et al., 2005; Soares et al., 2018
Chrysoporthe inopina	Pyriform to pulvinate	70-710	unilocular or multilocular	Oblong	3.0-4	1.5-2.5	11-29.5	Absent	Gryzenhout et al., 2006
Chrysoporthe hodgesiana	Pulvinate to pyriform	145-635	unilocular or multilocular	Oblong	3-5.5	1.5-2.5	12-33.0	Absent	Gryzenhout et al., 2004
Chrysoporthe deuterocubensis	Pyriform, clavate to pulvinate	100-950	unilocular or multilocular	Oblong	3-5.0	1.5-2.5	12-24.5	Absent	van der Merwe et al., 2010
Chrysoporthe cubensis	Pyriform to clavate	100-950	unilocular or multilocular	Oblong	2.5-5	1.5-3	10-26.5	Absent	Gryzenhout et al., 2004; Soares et al., 2018;
Chrysoporthe puriensis	Pyriform to pulvinate	95-470	unilocular or multilocular	oblong, fusoid to oval	3-6.5	1.5-2.5	9.0-17	Present	Oliveira et al., 2021
Chrysoporthe syzygiicola	Globose	250-500	unilocular	Oblong to oval	2.0-4	1-2.0	11-13.5	Absent	Chungu et al., 2010
Chrysoporthe zambiensis	Rostrate to globose	208-310	unilocular	Oblong	2.5-4	1-2.0	14.0-17.5	Absent	Chungu et al., 2010
Chrysoporthe austroafricana	Pyriform to clavate	80-120	unilocular or multilocular	Oblong to oval	3-3.5	1.5-2	7.5-28	Absent	Gryzenhout et al., 2004; Heath et al., 2006

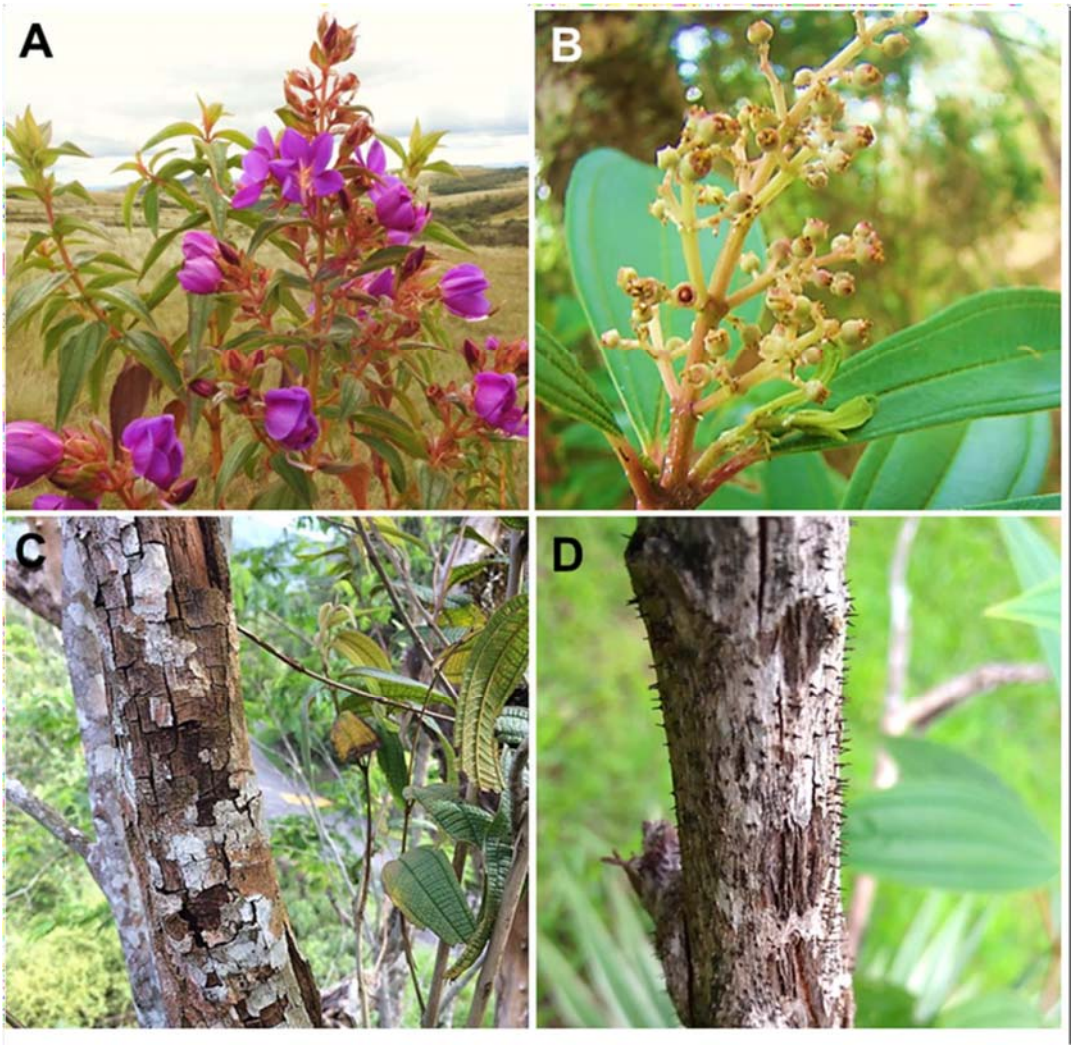

Fig. 1. Hosts and symptoms associated with infection by *Chrysoporthe brasiliensis*. (**A**) *R. grandiflora*. (**B**) *Miconia theaezans*. (**C**) *Miconia ibaguensis* with cracked bark associated with infection. (**D**) Pycnidia of *C. brasiliensis* produced on *R. grandiflora* infected branch.

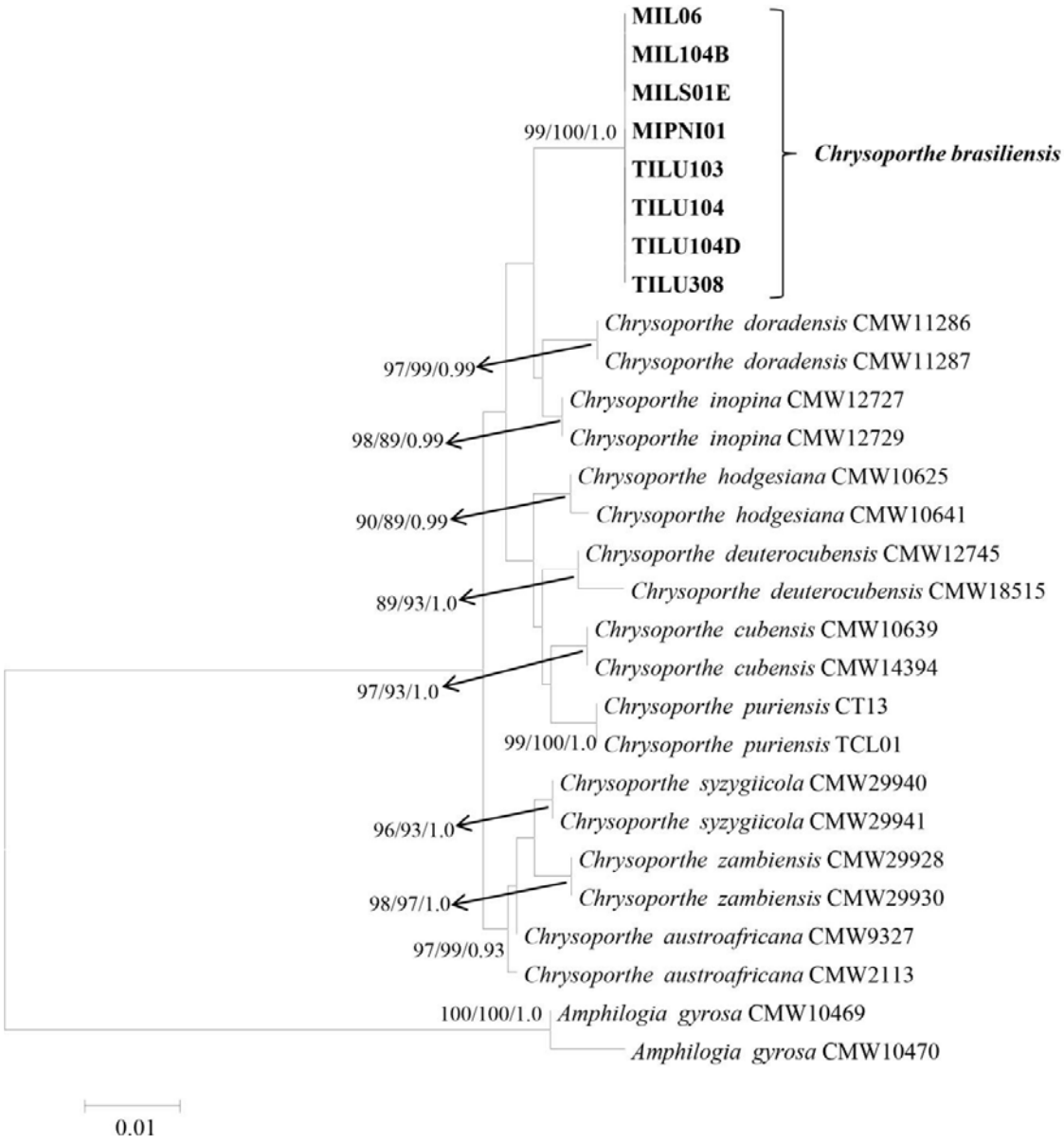

Fig. 2. Phylogenetic tree generated for the combined BT1, BT2, and ITS regions using a likelihood method. The bootstrap/posterior probability values are shown in the branches according to the maximum likelihood, maximum parsimony, and Bayesian inference analyses. *Amphilogia gyrosa* was used as the outgroup. The isolates of *Chrysoporthe brasiliensis* sp. nov. included in this study are highlighted in bold.

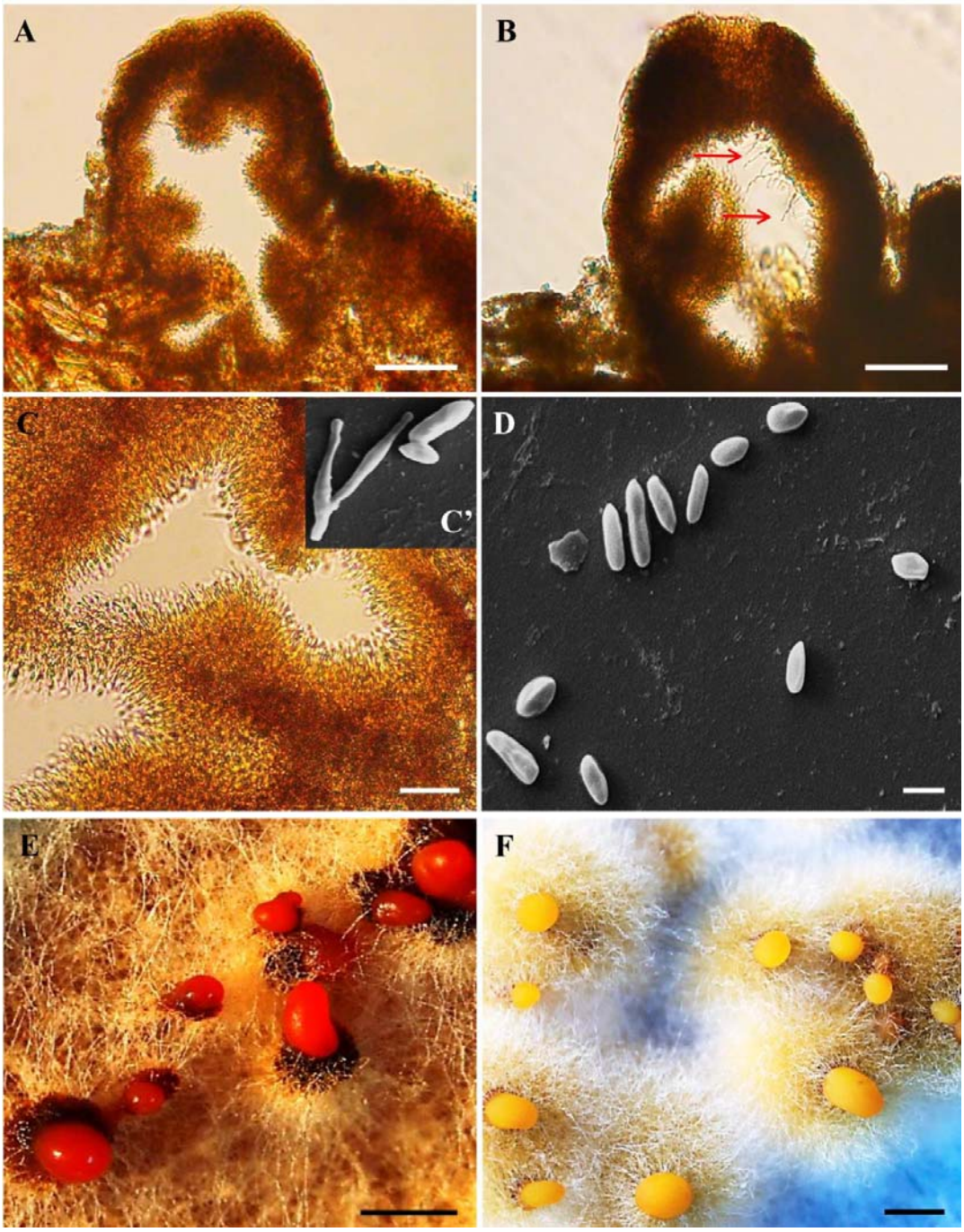

671

672 **Fig. 3.** Pycnidia, conidiogenous cells, conidia, and culture characteristics of
673 *Chrysoporthe brasiliensis.* (**A**) Pycnidium with a single convoluted locule. (**B**)
674 Pycnidial locule with paraphyses (indicated by red arrows). (**C**) Inner lining of pycnidial
675 locule with conidiogenous cells. (**D**) SEM showing variable sizes of conidia. (**E-F**)

Conidial masses at the apices of pycnidia on PDA after approximately 30 days of incubation. Scale bars: A and B= 50 µm; C= 20 µm; D= 2 µm; E and F= 500µm.

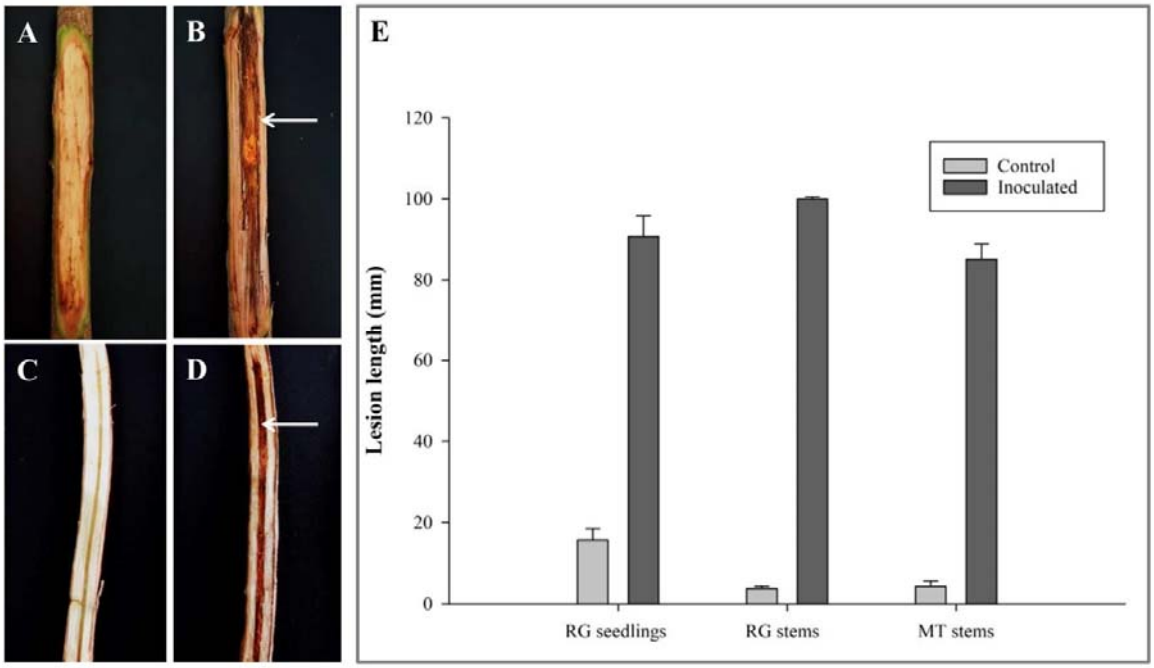

Fig. 4. Lesions on *R. grandiflora* (RG) and *Miconia theazans* (MT) after inoculation with *C. brasiliensis*. (**A**) *M. theaezans* stem section control and (**B**) inoculated. (**C**) *R. grandiflora* stem section control and (**D**) inoculated. White arrows denote necrotic lesions. (**E**) Mean lesion lengths (mm) on seedlings of *R. grandiflora* (after 60 days) and stem sections of *R. grandiflora* and *M. theaezans* (after 21 days) inoculated with *C. brasiliensis*. Media standard error bars.

8. Supplementary material

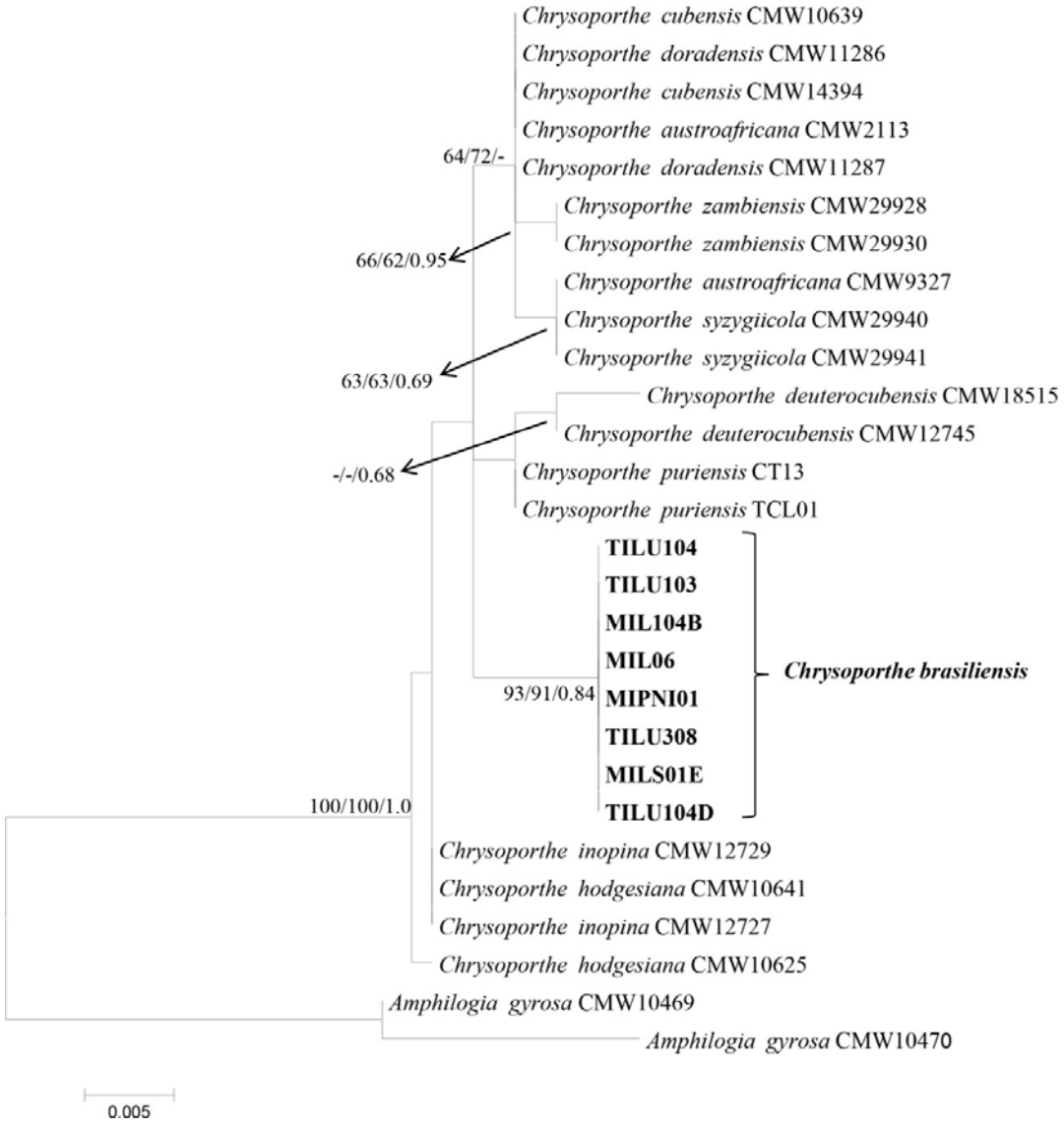

Figure 1S. Phylogenetic tree generated for the ITS region using a likelihood method. The bootstrap values >60% to maximum likelihood and maximum parsimony and posterior probability values >0.6 in Bayesian inference analyses are shown for the branches. *Amphilogia gyrosa* was used as the outgroup. The isolates of *Chrysoporthe brasiliensis* sp. nov. included in this study are presented in bold.

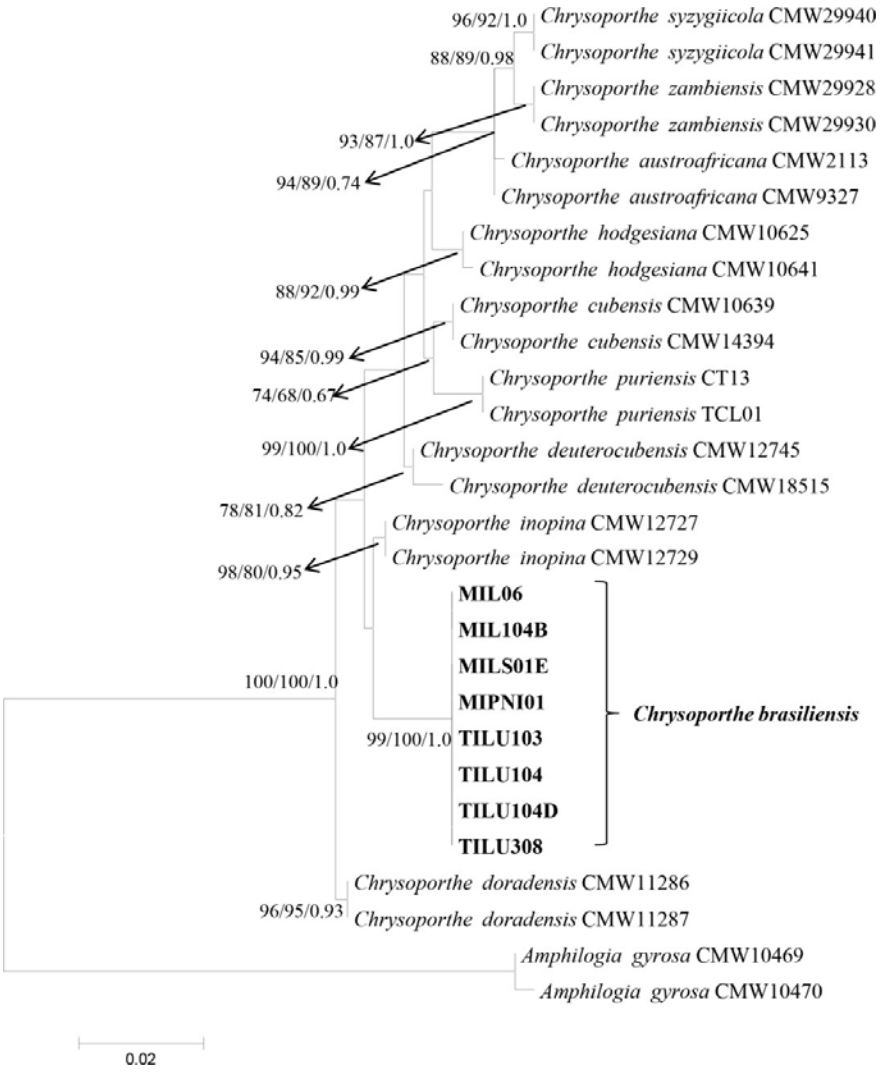

724

725 Figure 2S. Phylogenetic tree generated for the *β – tubulin* gene using a likelihood
726 method. The bootstrap/posterior probability values are shown for the branches
727 according to the maximum likelihood, maximum parsimony, and Bayesian inference
728 analyses. *Amphilogia gyrosa* was used as the outgroup. The isolates of *Chrysoporthe*
729 *brasiliensis* sp. nov. included in this study are presented in bold.

730